Brazilian Journal
of Chemical
Engineering

ISSN 0104-6632
Printed in Brazil
www.abeq.org.br/bjche

Vol. 36, No. 04, pp. 1475 - 1485, October - December, 2019
dx.doi.org/10.1590/0104-6632.20190364s20190268

NUMERICAL AND EXPERIMENTAL INVESTIGATION OF AIR-WATER SYSTEM TO SIMULATE BUBBLE DYNAMICS IN LIQUID SODIUM POOL

Arjun Pradeep[1], Anil Kumar Sharma[1*], M. P. Rajiniganth[1], N. Malathi[1], M. Sivaramakrishna[1], D. Ponraju[1], B. K. Nashine[1] and P. Selvaraj[1]

[1] Indira Gandhi Centre for Atomic Research, Kalpakkam, Tamil Nadu, India, E-mail: aksharma@igcar.gov.in - ORCID: 0000-0002-7420-7982

(Submitted: May 30, 2019 ; Revised: August 19, 2019 ; Accepted: August 31, 2019)

Abstract - The dynamics of rising bubbles in a liquid sodium pool plays a significant role in the estimation of the radiological source term during anticipated transients and normal operation of a fast reactor. Sodium is chemically reactive with air and water. Therefore, carrying out experiments using sodium on a reactor scale level requires extra precautions. We report an in-house experimental technique to depict the bubble dynamics along with numerical support to establish similarity behavior between water and liquid sodium, to reduce the number of experiments in sodium systems for in-depth knowledge of bubble dynamics in the case of the fast breeder reactor. In the present work, 3-D bubble dynamics is studied in the OpenFOAM platform and the validated numerical model is used to study bubble dynamics in sodium to establish similitude between the water and sodium systems. The bubble aspect ratio of 0.9 cm diameter bubbles in the sodium system is found to be in close agreement with that of 0.5 cm bubbles in the water system. Experimental and numerical findings suggest similarity of the aspect ratio between water and scaled-up sodium systems. The similarity criteria established between water and sodium are found to be very useful in conducting water-based experiments to study bubble dynamics in sodium systems.
Keywords: Bubble dynamics; OpenFOAM; Terminal velocity; Void sensors.

INTRODUCTION

Bubble movements can be originated during the entrainment of cover gas, fission gases or sodium vapor in a liquid sodium pool during anticipated transients of a fast breeder reactor (Henry et al., 1971). The rising bubble dynamics play a vital role in the stable operation of reactors and also in radiological source term estimation during anticipated transients. The characteristics of bubbles can be better predicted from gas release tests rather than tests using single bubbles (Dickinson and Nunamaker, 1975). However, the understanding of single bubble rise dynamics is of major importance towards understanding complex bubbly flows involved in the gas release tests. Experimentally, it is difficult to study the dynamics in sodium systems, due to issues associated with the handling of liquid sodium and its opaque nature. Wang (2015) carried out a numerical simulation on 2-D bubble dynamics and emphasized the need for experimental studies using suitable simulated studies.

Few experimental studies related to understanding bubble dynamics in sodium using water systems are available in the literature (Dickinson and Nunamaker, 1975; Quarterly Technical Progress Report, 1976). The bubble sizes in the simulated water experiment related to Sodium-cooled Fast Reactor (SFR) radiological source term safety studied at Hanford Engineering Development Laboratory (HEDL) ranged from 0.5 cm to 2.54 cm (Dickinson and Nunamaker, 1975). Based

* Corresponding author: Anil Kumar Sharma - E-mail: aksharma@igcar.gov.in

on the matching of dimensionless numbers, the typical bubble diameter predicted for a sodium pool is found to be 1.27 cm. From the bubble dynamics studies in the water system at HEDL, bubble sizes ranging from 1.1-4.1 cm in a sodium pool were studied experimentally at Atomic International. For radiological source term evaluation studies related to fast reactors, single bubble dynamics is typically studied for bubble sizes in the range 1-3 cm in a sodium pool based on fluid properties (Pradeep and Sharma, 2018; Miyahara et al., 1996; Miyahara and Sagawa, 1996). Pradeep and Sharma (2018) theoretically predicted the bubble size in sodium systems based on correlations developed by Levich (1962) and Park et al. (2017). Miyahara et al. (1996) carried out experiments in water to simulate bubble dynamics in a sodium system based on dimensionless number similarity criteria. It is clear from the literature that the theoretical studies related to establishing similarity between water and sodium systems based on bubble dynamics are scarce.

Even though similarities in bubble dynamics between sodium and water systems are reported in the literature, a quantitative analysis is missing in most of the studies. Several computational fluid dynamic (CFD) studies related to bubble rise in a liquid pool exist in the open literature (Krishna and Van Baten, 1999; Islam et al., 2013; Zahedi et al. 2014). Most of these studies are carried out using commercial software platforms such as Fluent, CFX. Few studies exist in the literature which use the open-source software OpenFOAM for such kind of simulations (Pradeep and Sharma, 2019). However, the OpenFOAM based studies were restricted to either 2-D or 2-D axisymmetric systems for the bubble dynamics problems studied to date (Samkhaniani et al., 2012; Raees et al., 2011, Pradeep et al., 2017), which under-predicted the bubble rise velocities and were not supported by experiments. Hence, OpenFOAM-based studies are required to simulate realistic bubble dynamics in water and sodium systems for three-dimensional computational domains.

Therefore, in the present work, 3-D numerical and experimental studies are judiciously combined for the first time to establish the quantitative nature of similarity in bubble dynamics between water and liquid sodium systems. The numerical study for simulating 3-D bubble dynamics is carried out using the OpenFOAM-based two-phase flow solver, interFoam. Based on the numerical work carried out, a similarity criterion is proposed to set up an experimental facility for studying the bubble dynamics in sodium systems using water as the working fluid. The bubble terminal velocity is measured using void sensors positioned in the water pool for equivalent diameters ranging from 0.5-2.25 cm. Bubble movement is also recorded by using a video camera to visualize its shape while in movement up to the free surface. In-house generated experimental results are used to validate existing theoretical correlations and numerical predictions. The study provides insight on open-source numerical methods to capture bubble dynamics and an innovative technique to measure bubble velocity in large pools of fluids using in-house developed void sensors.

EXPERIMENTAL

Under the fission gas release scenario in FBRs, it is sufficient to equate Froude and Weber numbers of water and liquid sodium systems to obtain the dimensionless number similarity criteria (Dickinson and Nunamaker, 1975).

Equating Froude numbers for water and sodium systems

$$\frac{u_{water}^2}{d_{water}g} = \frac{u_{sodium}^2}{d_{sodium}g} \tag{1}$$

Equating Weber numbers for water and sodium systems

$$\frac{\rho_{water}u_{water}^2 d_{water}}{\sigma_{water}} = \frac{\rho_{sodium}u_{sodium}^2 d_{sodium}}{\sigma_{sodium}} \tag{2}$$

The similarity criteria depend on the mass and momentum transport properties of water and liquid sodium (Pradeep et al., 2017). Table 1 gives the mass and momentum transport properties of water and liquid sodium.

From equations (1) and (2),

$$d_{water} = d_{sodium}\sqrt{\frac{\sigma_{water}\rho_{sodium}}{\sigma_{sodium}\rho_{water}}} \tag{3}$$

The water bubble diameter equivalent to the sodium bubble diameter of 1-4.1 cm is ~0.58-2.38 cm according to this similarity criterion. However, the similarity between sodium and water systems has not been studied to date by considering the bubble aspect ratio as a suitable basis. Experiments are hence carried out in an in-house developed water setup to measure bubble characteristics, such as rise velocity and aspect ratio for establishing similarity criteria between sodium and water systems along with numerical

Table 1. Transport properties of water and liquid sodium.

Properties	Water	Sodium
T (K)	303	473
ρ_l (kg/m^3)	995	904.3
μ_l (kg/ms)	0.0008	0.0004
σ (N/m)	0.071	0.189

computations. Based on the established similarity criteria, experiments can be carried out in the water system to simulate the possible bubble diameters encountered in the sodium pool of a typical Fast Breeder Reactor. Conductance-based void sensors measure the bubble rise velocity and image analysis is used for measuring bubble aspect ratio. The details of the experimental methodology are described in the following sub-sections.

Experimental setup

An experimental facility is established to study bubble rise dynamics in the water system. The photograph of the facility is shown in earlier work (Pradeep et al., 2017). The vessel of dimensions 0.61 m length, 0.61 m width and 1.22 m height is filled with water up to a maximum height of 1.17 m from the vessel bottom. The vessel is made from transparent acrylic material to allow clear visualization of the bubble movement. A ladle comprising an acrylic cup with stainless steel shaft supported outside the vessel by a plummer block bearing acts as the bubble generating system. The shaft is mounted at a height of 0.22 m from the vessel bottom and can be rotated along its diameter. Air is introduced via a 0.006 m stainless steel tube nozzle provided exactly below the center of the cup at a height of 0.07 m above the vessel bottom. The other end of the air inlet tube is provided with a water leak-tight septum, which allows air injection from a syringe to the air inlet tube and prevents the reverse flow of water into the syringe. The air is made to trap inside the cup such that, when rotated, a single bubble is produced. The equivalent diameter of the generated bubble is obtained from the volume of air injected using the graduated syringe.

Sensing methodology

Voids can be detected in a two-phase (air and water) medium by different means, which include, sensing the resistance offered by the bubbles in the conductance path, the capacitance change caused by the bubbles while passing through the capacitor arrangement, or through change in magnetic property of the medium when bubbles pass through an inductor. The inherent property of the fluid and the bubble dynamics determine which type of sensor can be used for detecting the velocity of the rising bubble. Considering the property of the working fluid (water), it was decided to use the conductance-based sensing methodology to get better detection capability and repeatability compared to other sensing methodologies. The conductance-based sensors designed for detecting bubbles are hereafter referred to as 'void sensors'. The uniqueness and strength of this sensing methodology lie in a precise detection of bubbles which is independent of its size, shape, and path of travel. Sensing the presence of a bubble is adequate to calculate the velocity of the bubble traveling at a certain speed by using two void sensors of the same type separated at a known distance. Bubble velocity measurement in a static pool can be carried out by measuring the travel time of the bubble between the two void sensors. As the bubble crosses between the sensing electrodes, a dip in conductance is observed. The time difference between two such dips from the two void sensors is calculated from the sensor output. Using the information of the calculated time difference in the basic equation of motion, the bubble velocity is obtained.

Sensor electronics

A new class of digital sensors known as pulsating sensors has been developed and deployed in many physico-chemical applications (Sahoo et al., 2010; Malathi et al., 2015; Praveen et al., 2010). Unlike other conventional sensors, the primary electronic response of the sensors is in pulse form, i.e., in the digital domain, which avoids intermediate signal processing stages of pre-amplification, post-amplification, and analog-to-digital conversion. Pulsating sensors have the flexibility in design, to use one of the four basic electrical properties: (i) resistance/resistivity (or conductance/conductivity), (ii) dielectric permeability, (iii) inductance, and (iv) electromotive force in a physical or physico-chemical system. Any parameter that causes any of the above properties to change, directly or indirectly, becomes measurable. These four different sensing parameters, individually or in combination, offer an extensive scope for monitoring a parameter redundantly. In each of these sensors, the signal output is a digital pulse frequency which carries information of the physical parameter being sensed. The relation between frequency and the sensed parameter is obtained by appropriate *in situ* calibration. The conductivity based sensor consists of a pair of electrodes placed in the sensing medium, which is a part of the timing circuit of a miniaturized resistance-capacitance type logic gate oscillator (LGO). The sensing electrodes constitute the resistance of the LGO. A fixed value capacitor is used in the timing circuit of the oscillator. The LGO oscillates between two logic states "0" and "1", when powered by 5V DC. The signal generated by LGO is a train of rectangular pulses of 5V amplitude from which the pulse frequency is determined. These digital pulses can be interfaced with any digital input/output card for further data processing without any auxiliary amplification or signal processing. Figure 1 depicts a simplified block diagram of the signal routing from the probe end to the Graphical user display in the PC.

Sensing probe construction

The main function of a void sensor is to detect the velocity at which a void rises in a static pool. Accordingly, the void sensing probe is designed in such

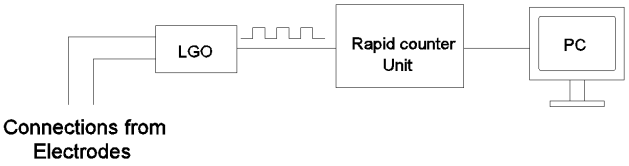

Figure 1. Block diagram of the signal path from probe to display in the PC.

a way that the sensor is immersed in the static pool. Since conductance-based void detection, in general, gives good results in such environments (Aggarwal et al., 2012), electrodes of different configurations are designed and optimized. The various configurations that were experimentally analyzed were mesh-type electrodes, ring-type electrodes, and wire-type electrodes. Wire-type electrodes were selected, and used for high sensitivity to avoid wall effects and to produce better results in terms of repeatability. In wire-type electrodes, it was found that the bubbles crossed the electrodes within a few milliseconds, which was less than the gate time. To increase the residence time of bubbles between the electrodes, the wire-type electrodes were bent to an angle of 45° in the area where the bubble is expected to rise. The probe material was chosen to be a pair of enamel coated copper wires of 2 mm diameter, placed parallel to each other. Wires were inserted inside a Teflon rod of 12 mm diameter to provide proper insulation and also to act as a fixture. Electrode fixture schematic is represented in fig. 2. The enamel was removed at the bent area of the wire-type electrode so that the bare copper facing each other forms the electrode pair, which is used as the void sensor. Two such electrode pairs were fixed one above the other at required distances depending on the water column height. The sensor was firmly secured with bolts at the top of the experimental vessel to avoid lateral movement of the sensor.

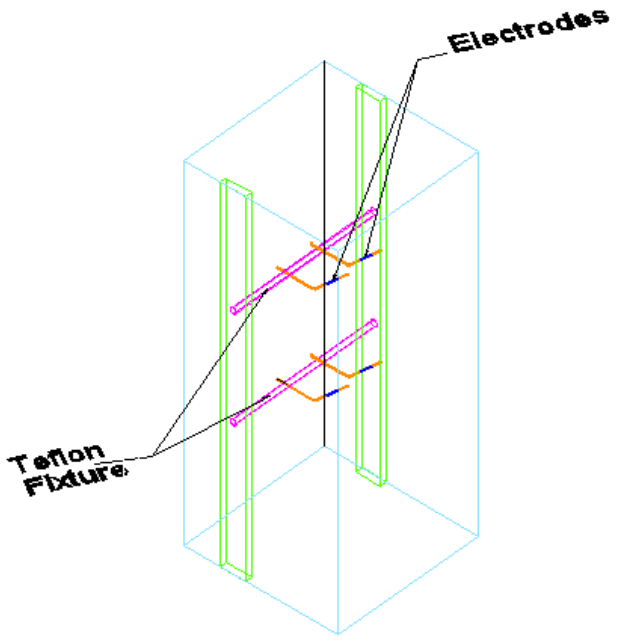

Figure 2. Schematic diagram of the electrode fixture.

The details of available theoretical correlations and the in-house numerical study used for characterizing bubble dynamics are presented in the following sub-sections.

THEORY

Correlations

The bubble dynamics are characterized by size, shape, and velocity. Correlations available in the literature for determining bubble terminal velocity require information on bubble shape and the shape determination requires information of bubble size. Several correlations (Davies et al., 1950; Mendelson, 1967; Talaia, 2007) are available in the literature for evaluating the terminal velocity of clean water and sodium as shown in Table 2. The relationship between bubble size and shape were given by Grace (1973) and Park et al. (2017) in terms of bubble shape diagrams. The bubble shape diagram encompasses the following non-dimensional numbers,

Morton number which depends on fluid properties is given by:

$$Mo = \frac{g\mu_l^4}{\rho_l \sigma^3} \tag{4}$$

The Eötvös number, which represents the ratio of gravitational to surface tension force, is given by:

$$Eo = \frac{g\rho_l d_B^2}{\sigma} \tag{5}$$

The Reynolds number, which represents the ratio of inertial to viscous force, is given by:

$$Re = \frac{d_B U_T \rho_l}{\mu_l} \tag{6}$$

Correlations (Taylor and Acrivos, 1964; Lee et al., 2014) are also available in the literature for evaluating the bubble aspect ratio of water, as shown in Table 3.

Numerical study

The open-source CFD software OpenFOAM 3.0.0 is used to simulate the behavior of a single bubble in a stagnant liquid. The simulations were performed in three-dimensional domains. The modified VOF based solver simulates the rise dynamics of a bubble composed of fluid 2 in a domain filled with fluid 1. The volume fraction α_1 is used to mark fluid 1 with the definition.

Table 2. Bubble terminal velocity correlations.

	Shape	Correlation
Davies and Taylor (1950)	spherical cap	$0.707\sqrt{gd}$
Mendelson (1967)	ellipsoidal	$\sqrt{\frac{2.14\sigma}{\rho_l d}+0.505gd}$
Talaia (2007)	spherical cap	$(0.691 \pm 0.021)\sqrt{\frac{gd\Delta\rho}{\rho_l}}$

Table 3. Bubble aspect ratio correlations.

	Correlation
Taylor and Acrivos (1964)	$\frac{1}{1+\frac{5}{32}We}$
Moore (1965)	$\frac{1}{1+\frac{9}{64}We}$
Lee (2014)	$\frac{1.7}{1+1.2Eo^{0.27}}$

$$\alpha_1 = \begin{cases} 1 & \text{in fluid 1} \\ 0 & \text{in fluid 2} \\ 0 < \alpha_1 < 1 & \text{at the interface} \end{cases} \quad (7)$$

The governing mass, momentum and volume fraction conservation equations for unsteady, laminar and incompressible Newtonian fluids in two-phase flow can be written as follows:

Continuity equation

$$\nabla \cdot \vec{u} = 0 \quad (8)$$

Momentum equation

$$\frac{\partial(\rho\vec{u})}{\partial t} + \nabla \cdot (\rho\vec{u}\vec{u}) = -\nabla p_{rgh} + \nabla \cdot (\mu \nabla \vec{u}) + \nabla \vec{u} \cdot \nabla \mu - \vec{g} \cdot \vec{x} \nabla \rho + \sigma\kappa\nabla\alpha_1 \quad (9)$$

Volume fraction equation

$$\frac{\partial \alpha_1}{\partial t} + \nabla \cdot (\vec{u}\alpha_1) + \nabla \cdot \left[\vec{u}_r \alpha_1 (1-\alpha_1)\right] = 0 \quad (10)$$

$$\rho = \alpha_1\rho_1 + (1-\alpha_1)\rho_2 \quad (11)$$

$$\mu = \alpha_1\mu_1 + (1-\alpha_1)\mu_2 \quad (12)$$

$$p_{rgh} = p - \rho\vec{g} \cdot \vec{x} \quad (13)$$

The interFoam solver available in OpenFOAM (Greenshields, 2016) uses the VOF method with surface compression approach for solving the governing conservation equations. The algorithm used for pressure velocity coupling is PIMPLE, a combination of PISO (Pressure Implicit with Splitting of Operators) and SIMPLE (Semi-Implicit Method for Pressure-Linked Equations) algorithms (Weller et al., 1998). The PIMPLE algorithm solves the pressure correction, the first pressure loop, the second and last pressure loops and the velocity equation. The Preconditioned Bi-Conjugate Gradient (PBiCG) with Diagonal Incomplete-Lower Upper (DILU) preconditioner is used for solving the velocity equation and the diagonal incomplete Cholesky (DIC) preconditioned CG is used for solving the pressure equations. The interface capturing algorithm used in interFoam is Multidimensional Universal Limiter with Explicit Solution (MULES). The machine used for computation is an Intel Core 2 Duo@2.4 GHz and 4 GB of RAM. The 3-D domain considered for the study initially consists of spherical bubble of diameter d_B positioned on the central vertical axis at an elevation of 0.5 d_B above the bottom wall. The gas bubble and liquid pool are considered to be in thermal equilibrium and the acceleration due to gravity is 9.81 m/s^2. The boundary conditions considered in the study are the wall for the bottom, side boundaries, and atmosphere for the top boundary.

The post-processing of numerical results is carried out using both ParaView and swak4Foam. The open-source data analysis and visualization application, ParaView 4.4 is used in the present study for obtaining the bubble contours. The swak4Foam library requires installation and compilation on the computer and allows a few conditions on the data extracted and specifying expressions involving the velocity fields. The ParaView is used to visualize fields for velocity and phase fraction, whereas the swak4Foam toolbox evaluates instantaneous rise velocity, the center of mass and bubble aspect ratio. The terminal rise velocity is obtained by averaging the values of rise velocity, which would not be expected to change with time (Rusten, 2013)."

Grid independence study

The dynamics for a 0.9 cm bubble is studied for the argon-sodium system in a 3-D cubic domain of dimensions $8d_B$ x $8d_B$ x $8d_B$. The study was carried out using three grids, coarse (112 x 112 x 112), medium (128 x 128 x 128) and fine (144 x 144 x 144). Figure 3 (a) shows that, in the case of rise velocity, the maximum percentage deviation of the medium grid from that of the coarse grid is 8.3 %, whereas it is only 3.4 % for the fine grid from the medium grid. Figure 3 (b) shows, in the case of center of mass, the maximum percentage deviation of the medium grid from that of the coarse grid is 1.3 %, whereas it is only 0.4 % for fine grid from the medium grid. Therefore, based on the grid independence study the medium grid (128 x 128 x 128) is chosen for the present analysis.

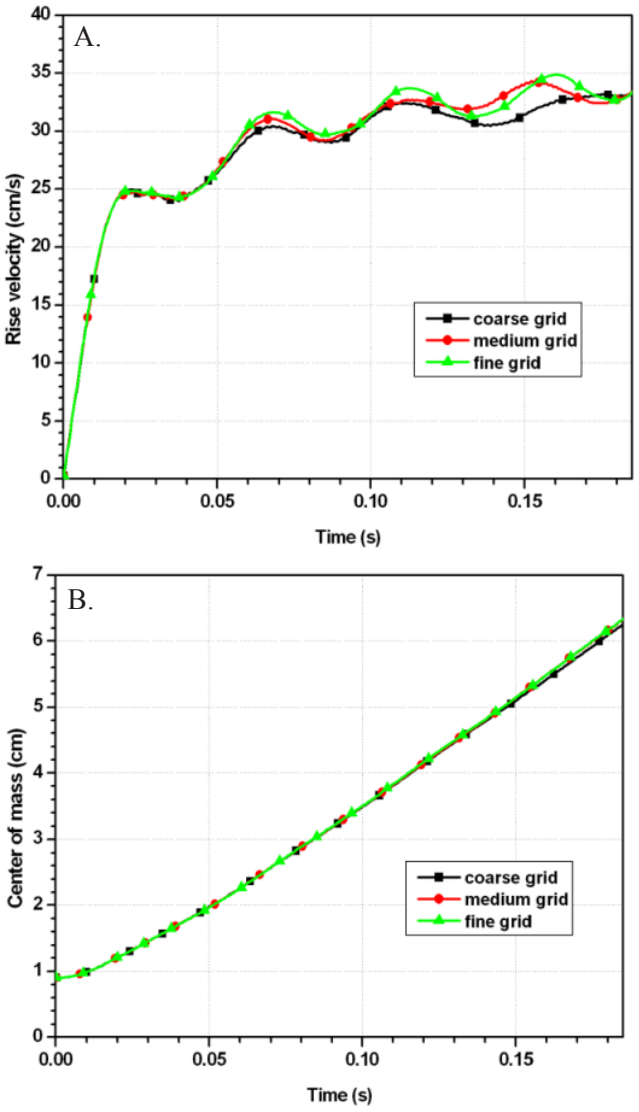

Figure 3. Grid independence study for an argon bubble rising in sodium (a) instantaneous rising velocity of the bubble (b) center of mass for the rising bubble.

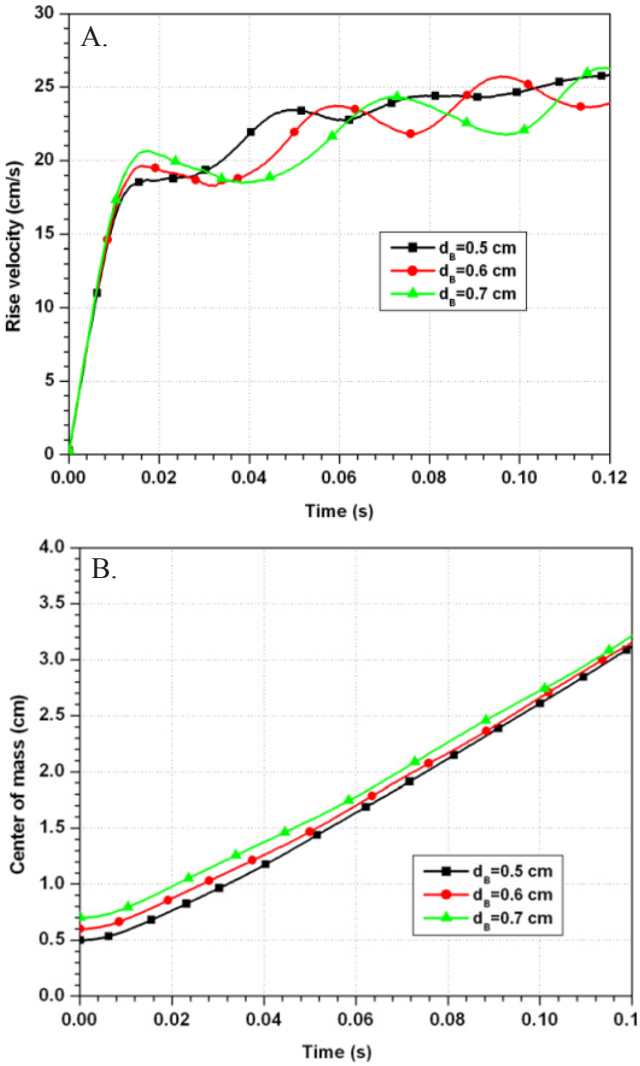

Figure 4. Effect of bubble diameter for an air bubble rising in water (a) bubble velocity (b) center of mass for the rising bubble.

Validation of the model

Validation of the numerical model has been carried out with in-house generated experimental data for the air-water system and the Mendelson correlation. The solution domain size is taken as $W = 8d_B$, so that the sidewall effect on the bubble behavior is negligible. To validate the 3-D numerical model for the water system, the temporal variations in bubble dynamics are studied as shown in Fig. 4 (a) and (b) for diameters ranging from 0.5-0.7 cm. The numerically predicted terminal velocity for 0.5 cm, 0.6 cm and 0.7 cm bubbles in water are obtained as 23.5 cm/s, 23.8 cm/s and 22.7 cm/s, respectively. The experimentally measured terminal velocity of a 0.5 cm bubble is 24.6 cm/s with an uncertainty of 2.5 cm/s. Figure 5 shows the validation of the numerically predicted terminal velocity for the air-water system with the in-house experiment and Mendelson correlation results. The numerically

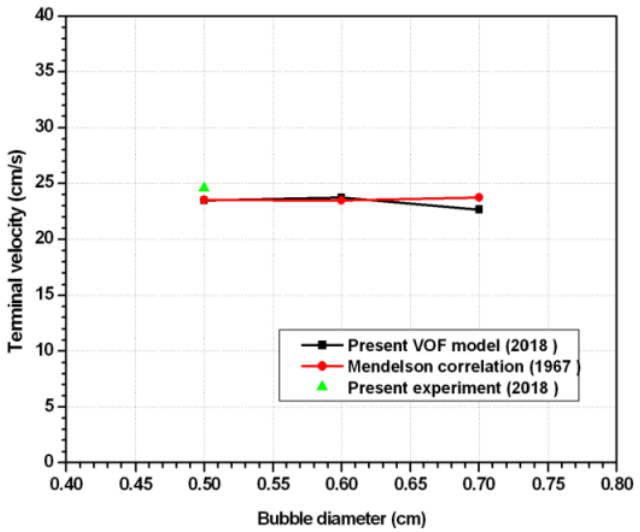

Figure 5. Validation of the present VOF model for the air-water system.

predicted terminal velocities are in close agreement with the Mendelson correlation and lower than the in-house experimental value by -4.5 % for the 0.5 cm bubble case. The numerically predicted aspect ratio of the 0.5 cm bubble in water is 0.62 and is in close agreement with the values of 0.624 obtained from the Taylor and Acrivos (1964) correlation and 0.6 obtained from the in-house experiment after thorough image analysis.

RESULTS AND DISCUSSION

Bubble dynamics in the sodium system: Numerical

After thorough numerical validation of the computational model using the in-house experiment as well as theoretical correlations available in the literature, systematic numerical analysis was carried out for an argon bubble rising in a sodium system. The vital results on the influence of different key parameters on bubble dynamics are discussed in the following sub-sections.

Effect of domain width

The solution domain width, *W* is varied from $6d_B$-$10d_B$, so that the sidewall effect on the bubble behavior can be studied. The temporal variations of the instantaneous rising velocity of the bubble and center of mass for a 0.9 cm argon bubble rising in sodium are shown in Fig. 6 (a) and (b), respectively. The bubble behavior is observed to be in close agreement for the three-domain widths studied. Hence, the study confirms that a domain width of $8d_B$ is sufficient to avoid a side wall effect.

Effect of domain height

The solution domain height, *H* is varied from $6d_B$-$10d_B$, so that the effect on the bubble behavior can be studied. Again, the temporal variations of bubble dynamics in terms of instantaneous rising velocity of the bubble and center of mass for a 0.9 cm argon bubble rising in sodium are shown in Fig. 7 (a) and (b), respectively. The bubble behavior is observed to be in close agreement for the three-domain heights studied. Hence, the study confirms that a domain height of $8d_B$ is sufficient for the bubble to reach terminal velocity.

Effect of bubble diameter

The solution domain size is taken as $8d_B$, so that the sidewall effect can be ignored. The temporal variations of bubble dynamics in terms of rise velocity of the bubble and center of mass for an argon bubble rising in sodium are shown in Fig. 8 (a) and (b) respectively. The numerically predicted terminal velocity for 0.9, 1 and 1.2 cm bubble diameters in sodium are found to be 30.2, 29.8 and 28.87 cm/s, respectively. The predicted terminal velocity is found to be lower than the value obtained from the Mendelson correlation by 6.9 % for the 1.2 cm bubble case (Fig. 9).

Similarity criteria between sodium and water: Numerical

Based on equating the dimensionless numbers, the similarity criteria between water and liquid sodium were obtained to date (Dickinson and Nunamaker, 1975). To simulate a bubble of specific diameter in the sodium system, the equivalent bubble diameter in the water system is ~0.58 of the corresponding diameter in the sodium system. Similarly, the terminal velocity obtained from the water experiment has to be divided by 0.76 to obtain the corresponding terminal velocity in the sodium system (Dickinson and Nunamaker, 1975; Pradeep et al., 2017). In this section, the bubble dynamics of a 0.5 cm bubble in the water system and

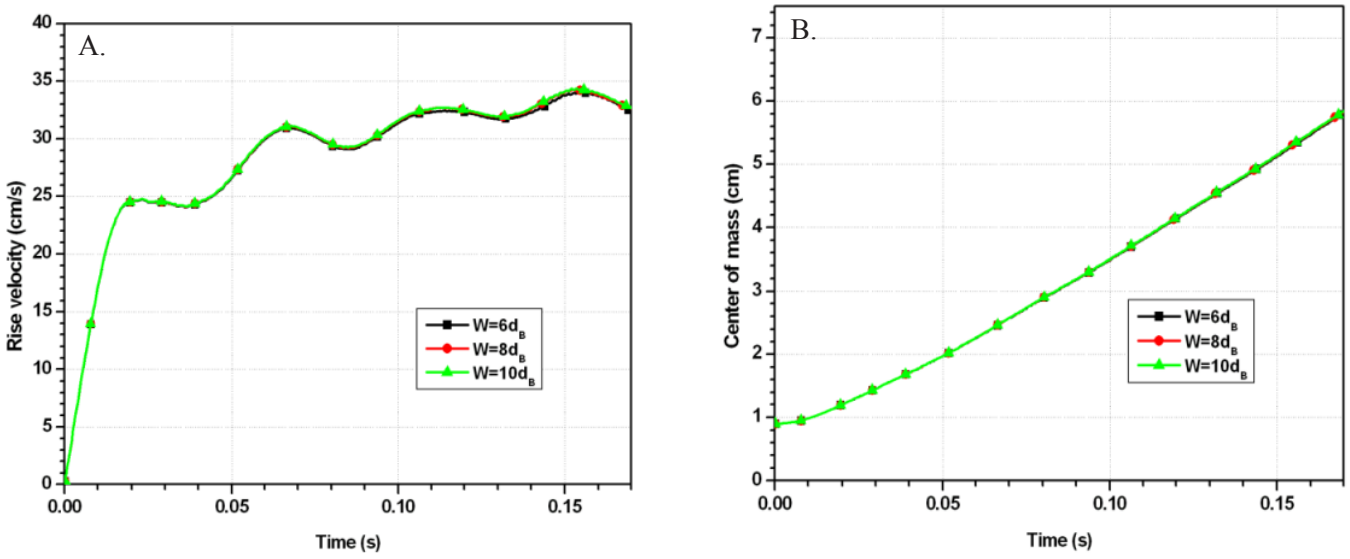

Figure 6. Effect of domain width for an argon bubble rising in sodium (a) instantaneous rising velocity of the bubble (b) center of mass for the rising bubble.

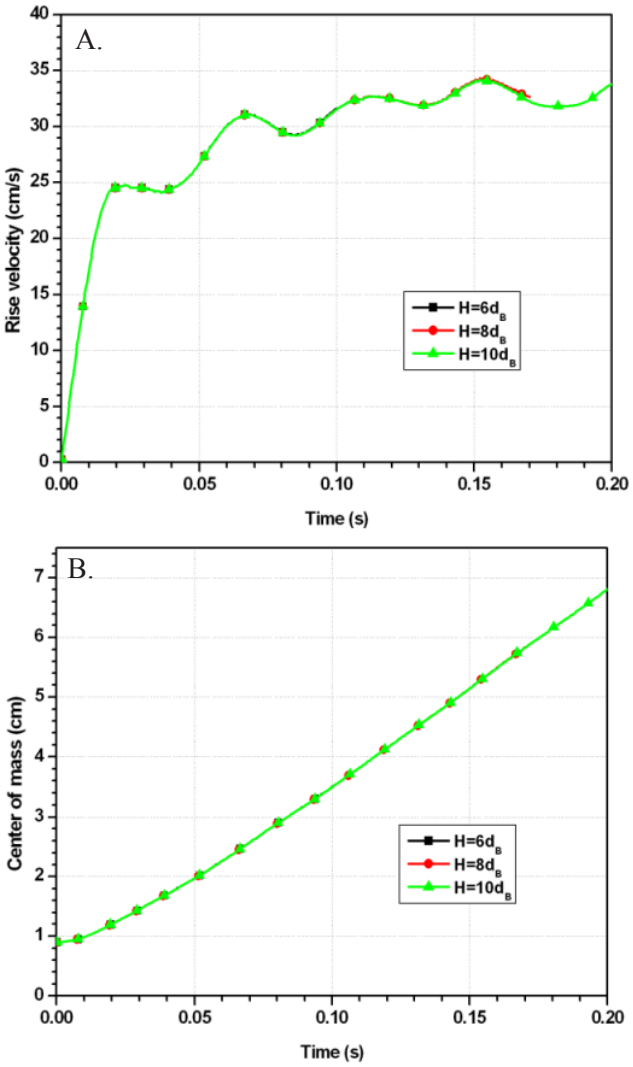

Figure 7. Effect of domain height for an argon bubble rising in sodium (a) instantaneous rising velocity of the bubble (b) center of mass for the rising bubble.

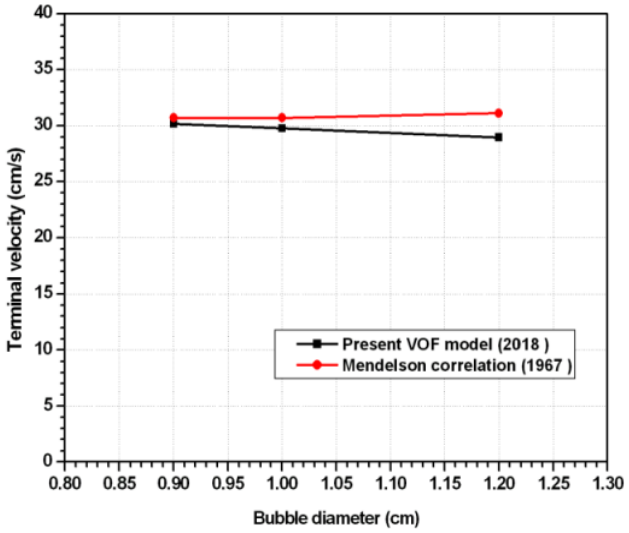

Figure 9. Terminal velocity predicted by the present VOF model and earlier correlations for the argon-sodium system.

a 0.9 cm bubble in the sodium system are compared numerically. The ratio of terminal velocities between the water system and sodium system is evaluated numerically as 0.77 and is in close agreement with that obtained from dimensionless numbers. Figure 10 shows the similarity in bubble contours obtained from the 3-D numerical simulation for the water and sodium systems. The aspect ratio of the 0.5 cm bubble in water and the 0.9 cm bubble in sodium is found to be 0.62 and 0.61 respectively (Fig. 11). It can also be seen that the bubble aspect ratio of the 0.9 cm bubble in the sodium system is in good agreement with that of the 0.5 cm bubble in water. The observed bubble sizes from similarity studies in the sodium and water systems fall in the spheroidal regime of the bubble shape diagram as shown in Fig. 12.

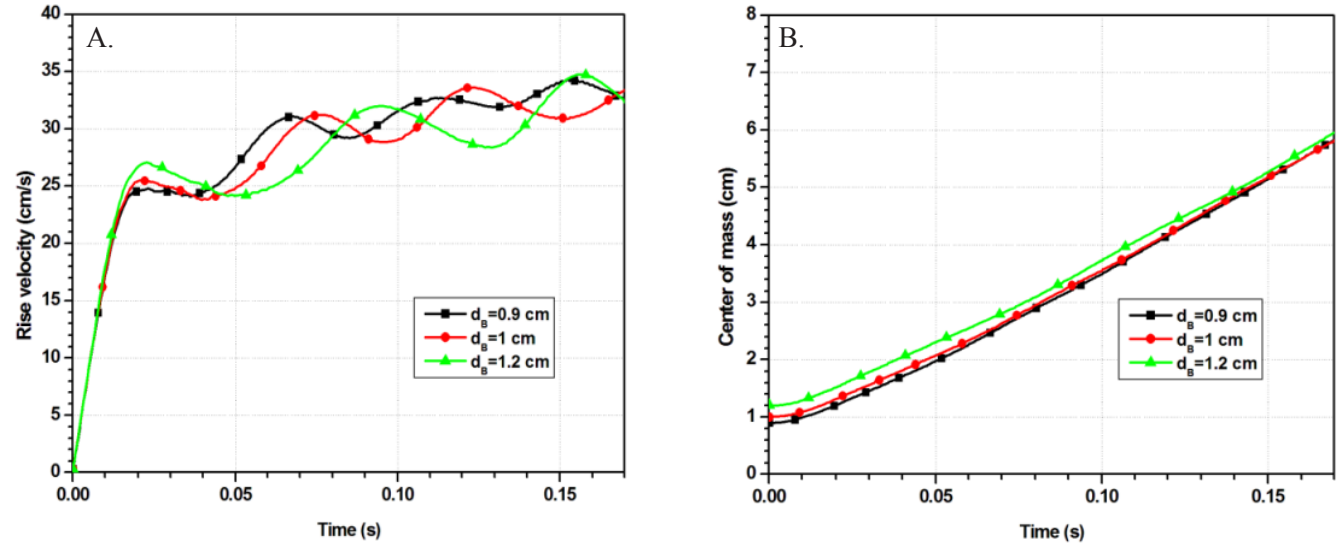

Figure 8. Effect of bubble diameter for an argon bubble rising in sodium (a) instantaneous rising velocity of the bubble (b) center of mass for the rising bubble.

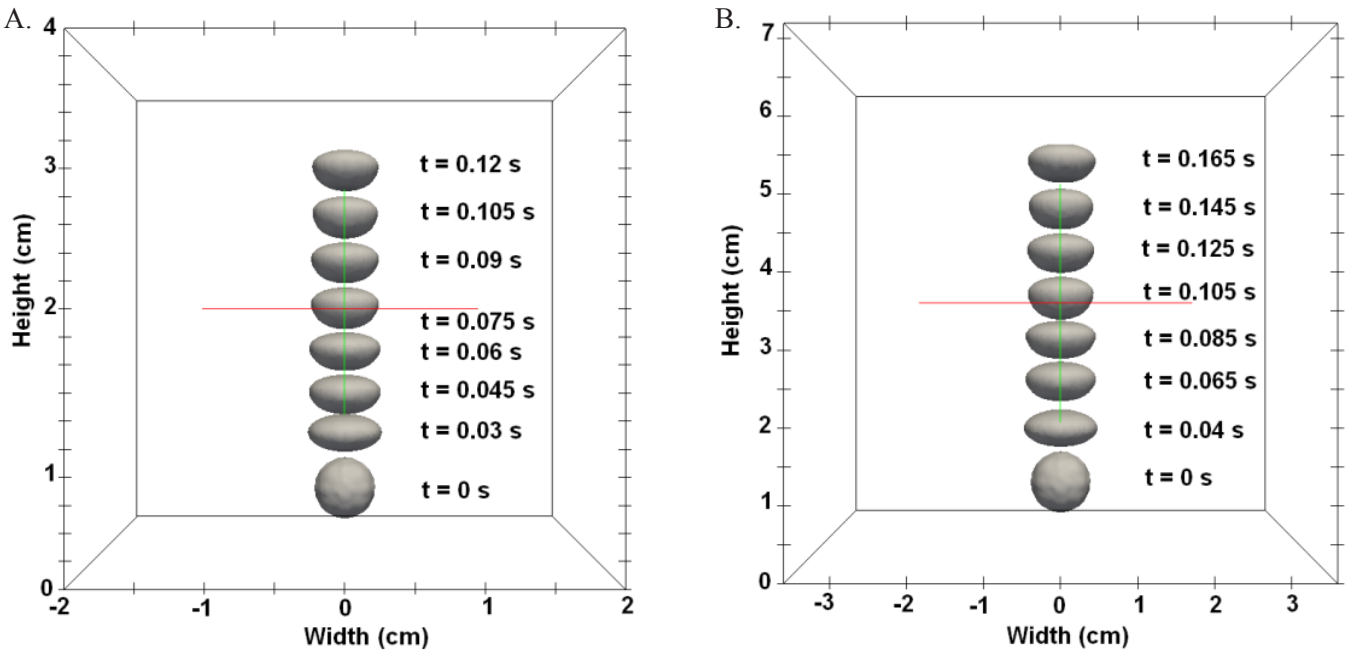

Figure 10. 3-D Numerical model for (a) a 0.5 cm bubble in water and (b) a 0.9 cm bubble in sodium.

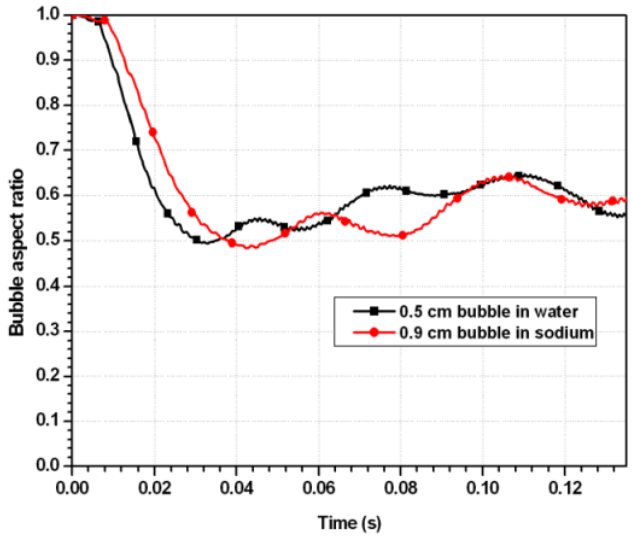

Figure 11. Simulation results for the aspect ratio for a rising bubble.

Hence, considering the similarity criterion established for medium to large-sized bubbles, a properly scaled-up water system can be used to simulate the sodium system for bubble dynamic studies related to SFR radiological source term evaluation.

Bubble dynamics in the water system: Experimental study to simulate the sodium system

Based on the similarity criteria developed between water and liquid sodium systems for bubble dynamics using the numerical two-phase model in the earlier section, an in-house experimental water setup was developed as already discussed for simulating the sodium system bubble dynamics. In-house bubble dynamic experiments measured the rise velocities of

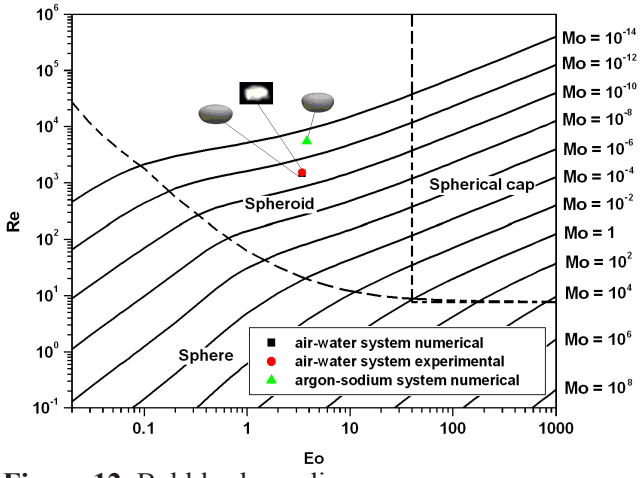

Figure 12. Bubble shape diagram.

bubbles in the range from 24.6 ± 2.5 cm/s to 29.1 ± 3.5 cm/s for equivalent diameters ranging from 0.5-2.25 cm respectively. Scaling up of the experimentally obtained bubble rise velocities in the water system for 0.5-2.25 cm diameters gives the rise velocities in the sodium system as 31.9-40.9 cm/s for diameters ranging from 0.84-3.8 cm in the sodium system. The results are in close agreement with the values of 30.8-44.7 cm/s predicted from the Mendelson correlation for the argon-sodium system. Since the equivalent diameter range of bubbles generated from the in-house water setup simulates the diameter range in the sodium studies (Quarterly Technical Progress Report, 1976; Pradeep and Sharma, 2018; Miyahara et al., 1996; Miyahara and Sagawa, 1996), the developed water set-up can be used to study bubble dynamics in a SFR pool related to in-vessel bubble transport source term studies.

CONCLUSION

A thorough understanding of bubble dynamics in liquid sodium has its importance in safety-related studies in the field of fast reactors. In the present work, we propose unique similarity criteria to use water as a working fluid for understanding bubble dynamics in liquid sodium systems by judiciously combining numerical and experimental studies for the first time. An in-house experimental setup is developed to study bubble dynamics in the water system. Experiments are carried out to understand the air bubble rise dynamics in the water column. A new class of digital sensors known as pulsating void sensors based on conductance measurements is used to measure the bubble velocity. The experimental data are used to validate the 3-D numerical model based on the open-source platform OpenFOAM 3.0.0 for bubble dynamics. The numerical model solves the governing equations for two-phase flow using a modified VOF method with a surface compression approach at the interface. The validated numerical model is used to study bubble dynamics in the sodium system and establish similitude between the water and sodium systems. The numerically predicted terminal velocity in the sodium system is found to be ~7 % lower than that obtained from the Mendelson correlation for a bubble diameter of 1.2 cm. The experimental and numerical study suggests similarity of the bubble aspect ratio between water and scaled up sodium systems. An excellent similarity of a water bubble of diameter 0.5 cm is observed with a sodium bubble with a 0.9 cm bubble diameter. Therefore, the established similarity criteria between water and sodium will be useful in conducting water-based experiments to study bubble dynamics in liquid sodium systems.

REFERENCES

Aggarwal, P. K., Pandey, G. K., Malathi, N., Arun, A. D., Ananthanarayanan, R., Banerjee, I., Sahoo, P., Padmakumar, G., Murali, N. Investigation of free level fluctuations in a simulated model of a sodium cooled Fast Breeder Reactor using pulsating conductance monitoring device. Annals of Nuclear Energy, 41, 87-96 (2012). https://doi.org/10.1016/j.anucene.2011.11.020

Davies, R. M., Taylor, G. The mechanics of large bubbles rising through extended liquids and through liquids in tubes. Proceedings of the Royal Society of London A: Mathematical, Physical and Engineering Sciences, 200, 375-390 (1950). https://doi.org/10.1098/rspa.1950.0023

Dickinson, D. R., Nunamaker, F. H. LMFBR source term iodine attenuation test of bubble breakup/coalescence in LMFBR outlet plenum following large fission gas release. No. HEDL-TC-537, Hanford Engineering Development Lab., Richland, Wash., USA (1975). https://doi.org/10.2172/7231204

Grace, J. R. Shapes and velocities of bubbles rising in infinite liquids. Transactions of the Institution of Chemical Engineers, 51, 116-120 (1973).

Greenshields, C. J. OpenFOAM user guide (2016).

Henry, R. E., Grolmes, M. A., Fauske, H. K. Pressure-pulse propagation in two phase one- and two- component mixtures. ANL-7792, Argonne National Laboratory, Illinois (1971). https://doi.org/10.2172/4043485

Islam, M. T., Ganesan, P., Sahu, J. N., Uddin, M. N., Mannan, A. A single air bubble rise in water: A CFD study. Mechanical Engineering Research Journal, 9, 1-6 (2013).

Krishna, R., van Baten, J. M. Rise characteristics of gas bubbles in a 2D rectangular column: VOF simulations vs experiments. International Communications in Heat and Mass Transfer, 26, 965-974 (1999). https://doi.org/10.1016/S0735-1933(99)00086-X

Lee, J. Y., Choi, Y. S. Lift Force of Large Bubble in High Reynolds Condition, 346-357 (2014).

Levich, V. G. Physiochemical Hydrodynamics. Englewood Cliffs, New Jersey, Prentice Hall (1962).

Malathi, N., Sahoo, P., Ananthanarayanan, R., Murali, N. Level monitoring system with pulsating sensor - Application to online level monitoring of dashpots in a Fast Breeder Reactor. Review of Scientific Instruments, 86, 025103 (2015). https://doi.org/10.1063/1.4906817

Mendelson, H. D. The prediction of bubble terminal velocities from wave theory. AIChE Journal, 13, 250-253 (1967). https://doi.org/10.1002/aic.690130213

Miyahara, S., Sagawa, N., Shimoyama, K. Iodine mass transfer from xenon-iodine mixed gas bubble to liquid sodium pool, (I) experiment. Journal of Nuclear Science and Technology, 33, 128-133 (1996). https://doi.org/10.1080/18811248.1996.9731874

Miyahara, S., Sagawa, N. Iodine mass transfer from xenon-iodine mixed gas bubble to liquid sodium pool, (II) Development of analytical model. Journal of Nuclear Science and Technology, 33, 220-228 (1996). https://doi.org/10.1080/18811248.1996.9731893

Moore, D. W. The velocity rise of distorted gas bubbles in a liquid of small viscosity. Journal of Fluid Mechanics, 23, 749-766 (1965). https://doi.org/10.1017/S0022112065001660

Park, S. H., Park, C., Lee, J., Lee, B. A simple parameterization for the rising velocity of bubbles in a liquid pool. Nuclear Engineering and Technology, 49, 692-699 (2017). https://doi.org/10.1016/j.net.2016.12.006

Pradeep, A., Sharma, A. K., Rajiniganth, M. P., Malathi, N., Sivaramakrishna, M., Ponraju, D., Nashine, B. K., Selvaraj, P. Bubble rise dynamics in water column, proceedings of the 24th National and 2nd International ISHMT-ASTFE Heat and Mass Transfer Conference, BITS Pilani, Hyderabad, India (2017).

Pradeep, A., Sharma, A. K. Semiempirical model for wet scrubbing of bubble rising in liquid pool of sodium-cooled fast reactor. Nuclear Engineering and Technology, 50, 849-853 (2018). https://doi.org/10.1016/j.net.2018.04.003

Pradeep, A., Sharma, A. K. Numerical investigation of single bubble dynamics in liquid sodium pool. Sādhanā, 44, 56 (2019). https://doi.org/10.1007/s12046-018-1041-5

Praveen, K., Rajiniganth, M. P., Arun, A. D., Ananthanarayanan, R., Malathi, N., Sahoo, P., Murali, N. High-performance differential pressure monitoring devices using pulsating sensors for a sodium-cooled fast breeder reactor. Nuclear Plant Operations and Control, 176, 127-137 (2010). https://doi.org/10.13182/NT11-A12547

Quarterly Technical Progress Report, Nuclear Safety, Characterization of Sodium Fires and Fast Reactor Fission Products. AI-ERDA-13172, Atomics International (1976).

Raees, F., van der Heul, D. R., Vuik, C. Evaluation of the interface-capturing algorithm of OpenFoam for the simulation of incompressible immiscible two-phase flow. Reports of the Department of Applied Mathematical Analysis, 11-07 (2011).

Rusten, E. S. A. Numerical study of the droplet-interface dynamic related to liquid-liquid separators. Master's thesis, Department of Physics, Norwegian University of Science and Technology (2013).

Sahoo, P., Malathi, N., Praveen, K., Ananthanarayanan, R., Arun, A. D., Murali, N., Swaminathan, P. High performance conductivity monitoring instrument with pulsating sensor. Review of Scientific Instruments, 81, 065109 (2010). https://doi.org/10.1063/1.3449552

Samkhaniani, N., Ajami, A., Kayhani, M. H., Dari, A. S. Direct numerical simulation of single bubble rising in viscous stagnant liquid, In International Conference on Merchanical, Automobile and Robotics Engineering (2012).

Talaia, M. A. Terminal velocity of a bubble rise in a liquid column. World Academy of Science, Engineering and Technology, 28, 264-268 (2007).

Taylor, T. D., Acrivos, A. On the deformation and drag of a falling viscous drop at low Reynolds number. Journal of Fluid Mechanics, 18, 466-476 (1964). https://doi.org/10.1017/S0022112064000349

Wang, X. Numerical simulation of two-dimensional bubble dynamics and evaporation. PhD thesis, KU Leuven Arenberg doctoral school (2015).

Weller, H., Tabor, G., Jasak, H., Fureby, C. A Tensorial Approach to CFD using Object Oriented Techniques. Computers in Physics, 12, 620-631 (1998). https://doi.org/10.1063/1.168744

Zahedi, P., Saleh, R., Moreno-Atanasio, R., Yousefi, K. Influence of fluid properties on bubble formation, detachment, rising and collapse; Investigation using volume of fluid method. Korean Journal of Chemical Engineering, 31, 1349-1361 (2014). https://doi.org/10.1007/s11814-014-0063-x